arXiv:cond-mat/0404428v2 [cond-mat.supr-con] 23 Apr 2004

2 February 2008

Oxygen-isotope effect on the in-plane penetration depth in cuprate superconductors

R. Khasanov†‡¶ , A. Shengelaya†, E. Morenzoni‡, K. Conder§, I. M. Savić‖, and H. Keller†

† Physik-Institut der Universität Zürich, CH-8057 Zürich, Switzerland

‡ Laboratory for Muon Spin Spectroscopy, Paul Scherrer Institut, CH-5232 Villigen PSI, Switzerland

§ Laboratory for Neutron Scattering, ETH Zürich and PSI Villigen, CH-5232 Villigen PSI, Switzerland

‖ Faculty of Physics, University of Belgrade, 11001 Belgrade, Serbia and Montenegro

Abstract. Muon-spin rotation (μSR) studies of the oxygen isotope (^{16}O/^{18}O) effect (OIE) on the in-plane magnetic field penetration depth λ_{ab} in cuprate high-temperature superconductors (HTS) are presented. First, the doping dependence of the OIE on the transition temperature T_c in various HTS is briefly discussed. It is observed that different cuprate families show a similar doping dependence of the OIE on T_c. Then, bulk μSR, low-energy μSR, and magnetization studies of the total and site-selective OIE on λ_{ab} are described in some detail. A substantial OIE on λ_{ab} was observed in various cuprate families at all doping levels, suggesting that cuprate HTS are non-adiabatic superconductors. The experiments clearly demonstrate that the total OIE on T_c and λ_{ab} arise from the oxygen sites within the superconducting CuO_2 planes, demonstrating that the phonon modes involving the movement of planar oxygen are dominantly coupled to the supercarriers. Finally, it is shown that the OIE on T_c and λ_{ab} exhibit a relation that appears to be generic for different families of cuprate HTS. The observation of these unusual isotope effects implies that lattice effects play an essential role in cuprate HTS and have to be considered in any realistic model of high-temperature superconductivity.

PACS numbers: 76.75.+i, 74.72.-h, 82.20.Tr, 71.38

¶ e-mail: rustem.khasanov@psi.ch

Present address: *Laboratory for Neutron Scattering, ETH Zürich and Paul Scherrer Institut, CH-5232 Villigen PSI, Switzerland; DPMC, Université de Genève, 24 Quai Ernest-Ansermet, 1211 Genève 4, Switzerland; Physik-Institut der Universität Zürich, Winterthurerstrasse 190, CH-8057 Zürich, Switzerland*

1. Introduction

Although the discovery of the cuprate high-temperature superconductors (HTS) [1] in 1986 triggered world-wide an enormous effort to understand these novel materials, there is at present still no convincing microscopic theory describing the mechanism of superconductivity. Due to the high values of the superconducting transition temperature T_c and the early observation of a tiny oxygen-isotope effect in optimally doped $YBa_2Cu_3O_{7-\delta}$ [2, 3, 4], many theoreticians came to the conclusion that the electron-phonon interaction cannot be responsible for high-temperature superconductivity. As a result, alternative pairing mechanisms of purely electronic origin were proposed. However, the assumption that T_c cannot be higher than 30 K within a phonon-mediated pairing mechanism is not justified [5]. A prominent example is the recent discovery of superconductivity in MgB_2 [6] with a $T_c \approx 39$ K which is accepted to be a purely phonon-mediated superconductor. There is increasing experimental evidence from recent work, such as neutron scattering [7, 8], angle resolved photoemission spectroscopy [9, 10], and isotope effect studies (this work) that lattice effects play an essential role in the basic physics of HTS and have to be considered in reliable theoretical models [11, 12].

It is well known that the observation of an isotope effect on T_c in conventional superconductors was crucial in the development of the microscopic BCS theory. The isotope shift may be quantified in terms of the relation

$$T_c \propto M^{-\alpha}, \qquad \alpha = -d\ln T_c/d\ln M\,, \tag{1}$$

where M is the isotope mass, and α is the isotope-effect exponent. In the simplest case of weak-coupling BCS theory $T_c \propto M^{-1/2}$ and $\alpha_{\rm BCS} \simeq 0.5$, in agreement with a number of experiments on conventional metal superconductors. However, there are exceptions of this rule such as Zr and Ru for which $\alpha \simeq 0$.

The conventional phonon-mediated theory is based on the Migdal adiabatic approximation in which the density of states at the Fermi level $N(0)$, the electron-phonon coupling constant λ_{ep}, and the effective supercarrier mass m^* are all independent of the mass M of the lattice atoms. However, if the interaction between the carriers and the lattice ions is strong enough, the Migdal approximation is no more valid [13]. Therefore, in contrast to ordinary metals, unconventional isotope effects on various quantities, such as the superconducting transition temperature and the magnetic penetration depth are expected for a non-adiabatic superconductor.

In 1990 the University of Zurich group started a project on isotope effect on cuprates that was initiated by K. Alex Müller. Here we briefly review some of our results. They include unconventional oxygen isotope ($^{16}O/^{18}O$) effects (OIE) in HTS on the transition temperature and the in-plane magnetic penetration depth. For a detailed description of our work we refer to Refs. [14, 15, 16, 17, 18, 19, 20, 21, 22]. In this review it is demonstrated that the muon spin rotation (μSR) technique is a very powerful and unique tool to investigate the OIE on the magnetic penetration depth in HTS. In particular, the novel low-energy μSR technique (LEμSR) [23] allows a direct and very

accurate measurement of the magnetic penetration depth in HTS and with that a reliable measurement of the OIE on λ.

The paper is organized as follows. In Sec. 2 we describe the sample preparation and the oxygen exchange procedure. Some results of the OIE on the transition temperature T_c obtained for different cuprate families are presented in Sec. 3. Sec. 4 comprises studies of the OIE on the in-plane penetration depth λ_{ab} in $Y_{1-x}Pr_xBa_2Cu_3O_{7-\delta}$ and $La_{2-x}Sr_xCuO_4$ by means of bulk μSR and in optimally doped $YBa_2Cu_3O_{7-\delta}$ by means of LEμSR . Furthermore, results of the site-selective OIE on λ_{ab} in $Y_{0.6}Pr_{0.4}Ba_2Cu_3O_{7-\delta}$ obtained by bulk μSR are reported. In Sec. 5 we discuss implications of the OIE on λ_{ab} and the empirical relation between the isotope effect on T_c and λ_{ab} observed for different HTS families. The conclusions follow in Sec. 6.

2. Sample preparation and oxygen isotope exchange

For isotope effect studies it is important to have isotope substituted samples of the same quality. In the case of $^{16}O/^{18}O$ oxygen substituted samples it means that both samples should have (i) exactly the same oxygen stoichiometry, (ii) the same oxygen distribution within the sample, and (iii) the same grain size distribution (in the case of powder samples). The schematic view of the experimental setup used for the oxygen

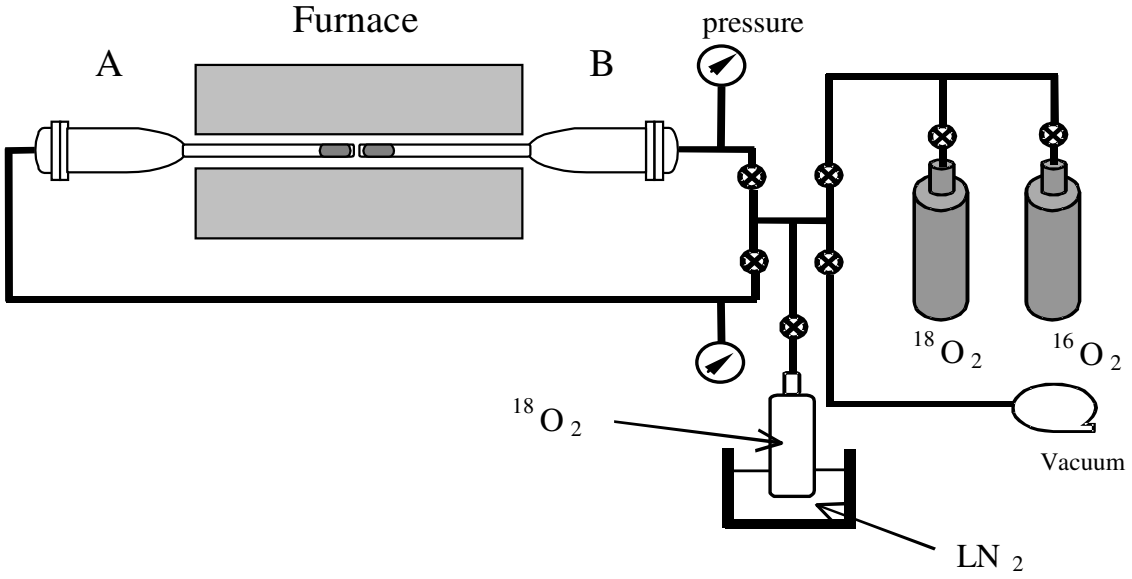

Figure 1. Experimental setup for preparation of the $^{16}O/^{18}O$ substituted samples.

isotope exchange is shown in Fig. 1 [24]. In order to ensure that the substituted samples are subject to the same thermal history, the annealing (in $^{16}O_2$ and $^{18}O_2$) is performed simultaneously. In chamber A the isotope exchange (^{18}O) and in chamber B an identical

process in normal oxygen (^{16}O) takes place. A liquid nitrogen trap is used to condense (and recycle) the expensive $^{18}O_2$ after the exchange process is finished. The exchange apparatus is equipped with a mass spectrometer (not shown), which allows to view the progress of the isotope exchange.

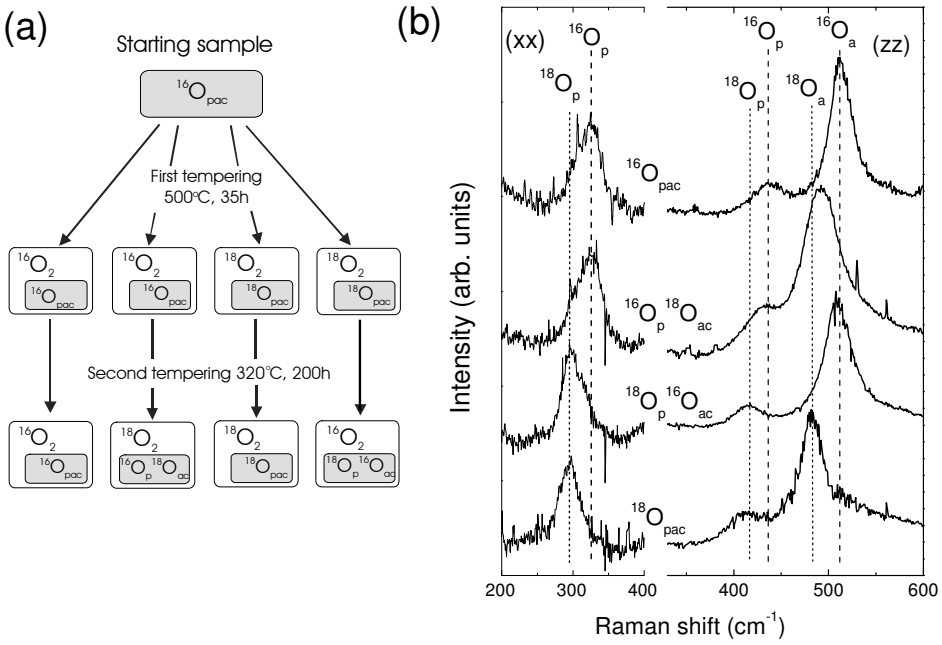

Figure 2. (a) Schematic diagram showing the oxygen isotope (^{16}O/^{18}O) substitution procedure to prepare completely and site-selective substituted samples. The first step is used to prepare completely oxygen substituted samples. The second step is used to prepare the site-selective samples from the completely substituted ones. (b) Room-temperature Raman spectra of the completely and site-selective oxygen substituted $Y_{0.6}Pr_{0.4}Ba_2Cu_3O_{7-\delta}$ samples. For xx polarization the line corresponds to the out-of-phase motion of the planar oxygen atoms (^{16}O, 325 cm^{-1}; ^{18}O, 294 cm $^{-1}$). For zz polarization the two lines correspond to the in-phase motion of the CuO_2 plane oxygen (^{16}O, 436 cm^{-1}; ^{18}O, 415 cm^{-1}) and to the bond-stretching mode of the apical oxygen (^{16}O, 512 cm^{-1}; ^{18}O, 482 cm^{-1}). After [21].

The procedure to prepare completely oxygen substituted and site-selective oxygen substituted $Y_{1-x}Pr_xBa_2Cu_3O_{7-\delta}$ samples (which are mostly described in this review) is schematically shown in Fig. 2(a). In the first step [500°C, 35 h at 1.2 bar in $^{16}O_2$ ($^{18}O_2$) gas] completely oxygen substituted samples ($^{16}O_{pac}$ and $^{18}O_{pac}$) are prepared. Here indexes p, a, and c stay for the planar (within CuO_2 planes), the apical and the chain oxygen, respectively. In order to prepare site-selective substituted samples after the first step they were grouped in two pairs. Then two site-selective samples ($^{16}O_p{}^{18}O_{ac}$ and $^{18}O_p{}^{16}O_{ac}$) were prepared via annealing one $^{16}O_{pac}$ sample in a $^{18}O_2$ atmosphere and one

$^{18}O_{pac}$ sample in $^{16}O_2$ gas (330°C, 150 h, 1.2 bar) [see Fig. 2(a)]. The other two samples (one $^{16}O_{pac}$ and one $^{18}O_{pac}$) were simultaneously annealed in the same atmosphere as before in order to have the reference samples following the same thermal history.

The results of the oxygen exchange can be checked by Raman spectroscopy. Fig. 2(b) shows Raman spectra with zz and xx polarizations of completely and site-selective oxygen substituted $Y_{0.6}Pr_{0.4}Ba_2Cu_3O_{7-\delta}$ samples [21]. In the $^{18}O_{pac}$ sample, the Raman lines are all shifted to lower frequencies in agreement with the results of Zech *et al.* [25], indicating a nearly complete exchange of ^{16}O with ^{18}O. In the site-selective sample $^{16}O_p{}^{18}O_{ac}$, only the position of the apical oxygen line is shifted to lower frequency, whereas the lines corresponding to the plane oxygen stay the same [apart from a small shift of one Raman line (433 cm^{-1} instead of 436 cm^{-1}), probably due to a small unintentional partial substitution by ^{18}O]. Note that the apical line (492 cm^{-1}) is also slightly shifted from the expected 482 cm^{-1}, indicating that the oxygen exchange for the apical and chain oxygen is slightly uncomplete. In the $^{18}O_p{}^{16}O_{ac}$ sample only the two planar lines are shifted, while the apical line stays the same.

3. Oxygen isotope effect on the transition temperature T_c

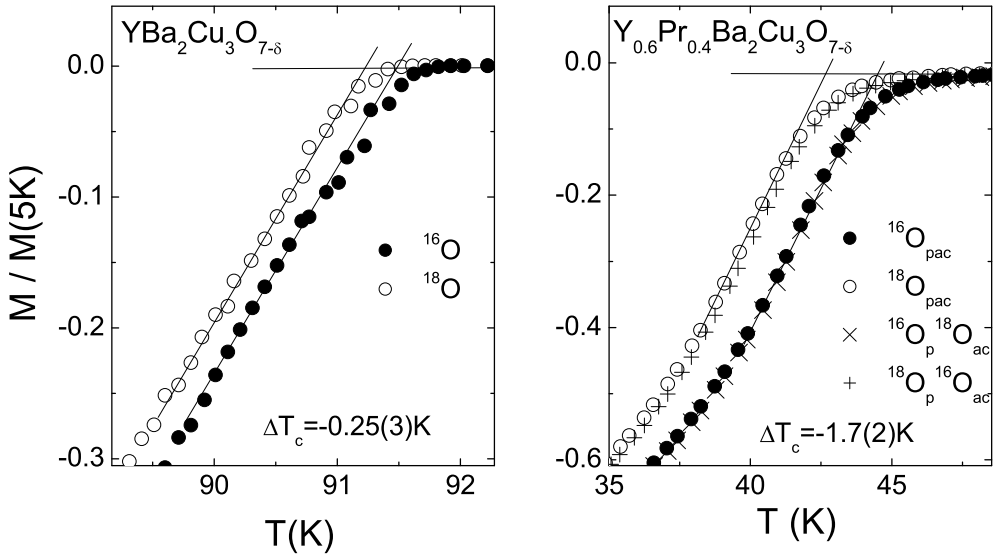

Figure 3. Section near T_c of the normalized (to the value at 5 K) magnetization curves (1 mT, FC) of the completely oxygen substituted $YBa_2C_3O_{7-\delta}$ (a) and the site-selective oxygen substituted $Y_{0.6}Pr_{0.4}Ba_2Cu_3O_{7-\delta}$ samples (b). After [21].

The importance of phonons for the pairing mechanism of conventional superconductors (including doped fullerenes [26] and MgB_2 [27]) was provided by

measurements of the isotope effect (IE) on T_c. The BCS theory predicts that

$$k_B T_c = 1.13\hbar\omega \exp\left(-\frac{1}{N(0)V}\right), \tag{2}$$

where ω is a typical phonon frequency (e.g. the Debye frequency ω_D). The electron phonon coupling is given by the product of the electron-phonon interaction constant V and the electronic density of states at the Fermi surface $N(0)$, both of which are assumed to be independent of the ion mass M. Eq. (2) implies an isotope-mass dependence of T_c ($T_c \propto \omega \propto 1/\sqrt{M}$), characterized by the isotope effect exponent $\alpha = 1/2$. This is in agreement with isotope effect results reported for many non-transition metal superconductors (e.g. Hg, Sn and Pd). However, as mentioned above, there are exceptions as Zr and Ru with $\alpha \simeq 0$.

Since 1987 a number of oxygen isotope effect investigations on T_c were performed in most families of HTS. The first OIE experiments were done on optimally doped samples, showing no significant isotope shift [2, 4]. However later experiments revealed a small but finite dependence of T_c on the oxygen isotope mass $M_{\rm O}$ [3, 28, 29]. It is now well established that the OIE on T_c is doping dependent [29, 30]. As an example, Fig. 3 shows the temperature dependence of the magnetization in the vicinity of T_c in optimally doped ^{16}O/^{18}O $YBa_2Cu_3O_{7-\delta}$ samples and site-selective oxygen exchanged $Y_{0.6}Pr_{0.4}Ba_2Cu_3O_{7-\delta}$ samples. It is seen that the isotope shift on T_c increases with decreasing doping (increasing Pr concentration) quite substantially: from ΔT_c=-0.25(3) K in optimally doped $YBa_2Cu_3O_{7-\delta}$ to ΔT_c=-1.7(2) K in highly underdoped $Y_{0.6}Pr_{0.4}Ba_2Cu_3O_{7-\delta}$.

The oxygen-isotope exponent $\alpha_O = -{\rm d}\ln T_c/{\rm d}\ln M_{\rm O}$ as a function of doping shows a trend that appears to be generic for all families of cuprate superconductors [15, 16, 18, 28, 31]. In the underdoped region α_O is large (even exceeding the BCS value α =1/2) and becomes small in the optimally doped and overdoped regime (see Fig. 4). Moreover, the copper-isotope (^{63}Cu/^{65}Cu) exponent $\alpha_{\rm Cu}$ shows a similar trend as $\alpha_{\rm O}$ [34, 35, 36, 37]. Both exponents increase monotonically with decreasing doping level (or T_c). For $Y_{1-x}Pr_xBa_2Cu_3O_{7-\delta}$ and $Y_{1-x}Pr_xBa_2Cu_4O_8$ close to optimal doping $\alpha_{\rm Cu} \simeq \alpha_{\rm O}$, whereas in the deeply underdoped regime $\alpha_{\rm Cu} \simeq 0.7\alpha_{\rm O}$ [18, 35, 36, 37].

The observation of OIE on T_c indicates that lattice vibrations in the CuO_2 planes are relevant for the occurrence of superconductivity. From this point of view, one would expect that the planar oxygen modes give rise to larger OIE on T_c than the apical and/or chain oxygen modes. The first reliable site-selective OIE (SOIE) studies of T_c were performed by Zech *et al.* [25]. It was shown that in optimally doped $YBa_2Cu_3O_{7-\delta}$ the planar oxygen mainly ($\geq$ 80 %) contribute to the total OIE on T_c. These results were confirmed by Zhao *et al.* [31] and later by Khasanov *et al.* [21]. Both groups [31, 21] found that in underdoped $Y_{1-x}Pr_xBa_2Cu_3O_{7-\delta}$ the predominant contribution (100 % within error bar) arises from the oxygen within the superconducting CuO_2 planes [see Fig. 3(b)].

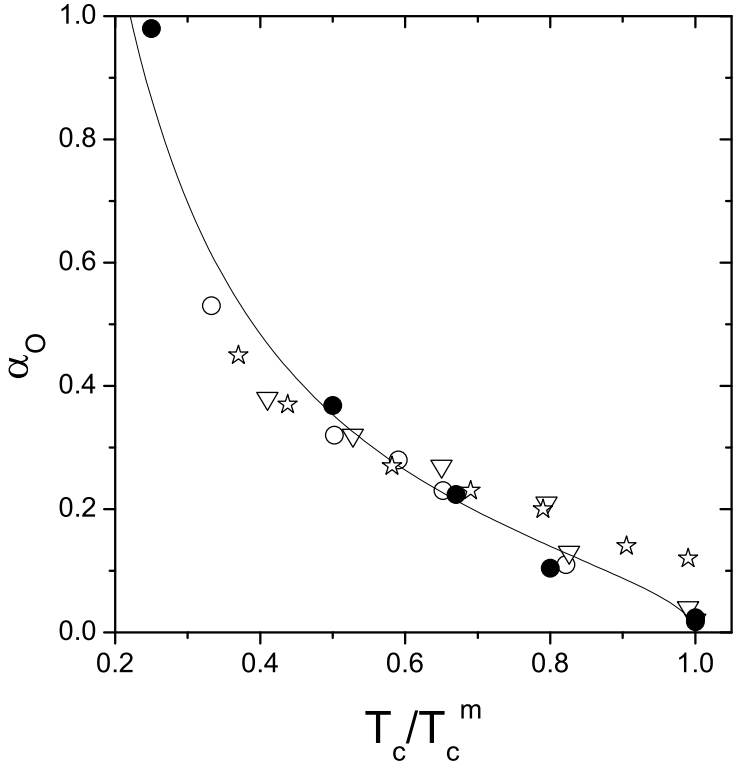

Figure 4. Oxygen isotope effect exponent α_O versus reduced temperature $\overline{T}_c = T_c/T_c^m$ (T_c^m is the maximum transition temperature of a given family of HTS). The open circles are $Y_{1-x}Pr_xBa_2Cu_3O_{7-\delta}$ data from [28]. Open down triangles are data of $YBa_{2-x}La_xCu_3O_7$ taken from [32]. Open stars are data of $La_{1.85}Sr_{0.15}Cu_{1-x}Ni_xO_4$ from [33]. Closed circles correspond to $Y_{1-x}Pr_xBa_2Cu_3O_{7-\delta}$ data from [20, 22] and unpublished data (this work). The solid line corresponds to $\alpha_O = 0.25\sqrt{(1-\overline{T}_c)/\overline{T}_c)}$ from [30].

4. Oxygen isotope effect on the in-plane magnetic penetration depth λ_{ab}

The conventional phonon-mediated theory of superconductivity (standard BCS theory) is based on the Migdal adiabatic approximation in which the effective supercarrier mass m^* is independent of the mass M of the lattice atoms. However, if the interaction between the carriers and the lattice is strong enough, the Migdal adiabatic approximation breaks down and m^* depends on M (see, *e.g.* [13]). A significant experiment to explore a possible coupling of the supercarriers to the lattice is an isotope effect study of the magnetic field penetration depth λ.

For a general Fermi surface the zero-temperature magnetic penetration depth $\lambda_{ii}(0)$ may be written as an integral over the Fermi surface [38]:

$$\frac{1}{\lambda_{ii}(0)^2} = \frac{\mu_0}{2\pi^2 h} \oint dS_F \frac{v_{F_i}\, v_{F_i}}{|v_F|}\,, \tag{3}$$

where i denotes the crystallographic axes (a, b, c) and v_{F_i} is the Fermi velocity. For the special cases of spherical or ellipsoidal Fermi surfaces, Eq. 3 leads to the London expression

$$\frac{1}{\lambda_{ii}(0)^2} = \mu_0 e^2 \frac{n_s}{m^*_{ii}}\,, \tag{4}$$

where n_s is the superconducting carrier density and m^*_{ii} is the effective mass of the carriers. For a general Fermi surface, it is convenient to *parameterize* experimental data by means of Eq. 4. It should be noted, however, that in this case m^*_{ii} is not directly related the band mass, except for spherical or ellipsoidal Fermi surfaces [38]. For HTS, which are superconductors in the clean limit, we may parameterize the in-plane penetration depth λ_{ab} in terms of the relation:

$$1/\lambda^2_{ab}(0) \sim n_s/m^*_{ab}\,, \tag{5}$$

where m^*_{ab} is the in-plane effective mass (not band mass) of the charge carriers. According to Eq. 5, this implies that an OIE on λ_{ab} has to be due to a shift in n_s and/or m^*_{ab}:

$$\Delta\lambda^{-2}_{ab}(0)/\lambda^{-2}_{ab}(0) = \Delta n_s/n_s - \Delta m^*_{ab}/m^*_{ab}. \tag{6}$$

Therefore a possible mass dependence of m^*_{ab} can be tested by investigating the isotope effect on λ_{ab}, provided that the contribution of n_s to the total isotope shift is known.

The first observation of a possible OIE on the magnetic penetration depth $\lambda(0)$ in polycristalline $YBa_2Cu_3O_{6.94}$ was reported by Zhao and Morris [39]. In another study Zhao *et al.* [40, 16] extracted the isotope dependence on $\lambda(0)$ in fine grained samples of $La_{2-x}Sr_xCuO_4$ ($0.06 \leq x \leq 0.15$) from the Meissner fraction. Hofer *et al.* [41] investigated the OIE on $\lambda^{-2}_{ab}(0)$ in tiny single crystals of $La_{2-x}Sr_xCuO_4$ by means of torque magnetometery. All these experiments showed indeed a pronounced oxygen isotope dependence of the magnetic penetration depth λ.

The μSR technique is a very powerful method to determine the magnetic penetration depth in superconductors. In the following we will discuss in more detail OIE investigations of λ_{ab} in optimally doped and underdoped cuprate HTS by means of bulk μSR and LEμSR, which at present is the most powerful and elegant technique to measure the magnetic penetration depth directly. Detailed bulk μSR investigations of polycrystalline samples of HTS have demonstrated that λ can be obtained from the muon-spin depolarization rate $\sigma(T) \sim 1/\lambda^2(T)$, which probes the second moment of the magnetic field distribution in the mixed state [42]. It was shown [43, 44] that in polycrystalline samples of highly anisotropic systems such as the HTS ($\lambda_c/\lambda_{ab} > 5$), $\lambda_{\rm eff}$ (powder awerage) is dominated by the shorter penetration depth λ_{ab} due to the supercurrents flowing in the CuO_2 planes: $\sigma(T) \propto 1/\lambda^2_{ab}(T)$. In LE$\mu$SR experiments spin-polarized low-energy muons are implanted in the thin film sample at a known depth z beneath the surface and precess in the local magnetic field $B(z)$. This feature allows to measure directly the profile $B(z)$ of the magnetic field inside the superconducting film in the Meissner state and to make a model independent determination of λ [45]. All the

OIE μSR results of T_c and λ_{ab} discussed in this review are summarized in Table 1. For comparison the low-field magnetization data are also included.

Table 1. *Summary of the OIE results.*

Compound	Method	Sample shape	$\Delta T_c/T_c$ (%)	$\Delta\lambda_{ab}(0)/\lambda_{ab}(0)$ (%)
$YBa_2Cu_3O_{7-\delta}$	LEμSR	thin film	-0.22(16)	2.8(7)
$YBa_2Cu_3O_{7-\delta}$	magnetization	fine powder	-0.26(5)	3.0(1.1)
			-0.28(5)[a]	2.4(1.0)[a]
$YBa_2Cu_3O_{7-\delta}$	bulk μSR	powder	-0.3(1)	2.6(5)
$Y_{0.8}Pr_{0.2}Ba_2Cu_3O_{7-\delta}$			-1.3(3)	2.4(7)
$Y_{0.7}Pr_{0.3}Ba_2Cu_3O_{7-\delta}$			-2.8(5)	2.5(1.0)
$Y_{0.6}Pr_{0.4}Ba_2Cu_3O_{7-\delta}$			-4.6(6)	4.5(1.0)
$La_{1.85}Sr_{0.15}CuO_4$			-1.0(1)	2.2(6)
$Y_{0.6}Pr_{0.4}Ba_2Cu_3O_{7-\delta}$	bulk μSR	site-selective	0.1(4)[b]	0.9(5)[b]
		powder	-3.7(4)[c]	3.1(5)[c]
			-3.3(4)[d]	3.3(4)[d]

[a] results for the back-exchange $^{16}O \rightarrow {}^{18}O$ and $^{18}O \rightarrow {}^{16}O$ samples

[b]results for the sample with ^{16}O at plane sites and ^{18}O at apical and chain sites

[c]results for completely ^{18}O substituted sample

[d]results for the sample with ^{18}O at plane sites and ^{16}O at apical and chain sites

4.1. OIE on λ_{ab} in underdoped region

The first measurements of OIE on $\lambda_{ab}(0)$ using bulk μSR were performed by Khasanov *et al.* [20] in underdoped $Y_{1-x}Pr_xBa_2Cu_3O_{7-\delta}$ ($x = 0.3$ and $x = 0.4$). The transverse-field μSR measurements were performed on the beam-line $\pi M3$ at the Paul Scherrer Institute (PSI, Switzerland) using low-momentum muons (29 MeV/c). The samples were field-cooled from far above T_c in a magnetic field of 200 mT. The depolarization rate σ was extracted from the μSR time spectra using a Gaussian relaxation function $R(t) \propto \exp(-\sigma^2 t^2/2)$. Above T_c a small temperature-independent depolarization rate $\sigma_{nm} = 0.15\ \mu s^{-1}$ is seen, arising from the nuclear magnetic moments. Below T_c, σ increases strongly due to the flux lattice formation. An additional sharp increase of $\sigma(T)$ was observed below 10 K which is due to antiferromagnetic ordering of Cu(2) moments [46]. However, zero-field μSR experiments indicate no presence of magnetism above 10 K. Therefore, data points below 10 K were excluded in the analysis. The

superconducting contribution σ_{sc} was then determined by subtracting σ_{nm} measured above T_c from σ.

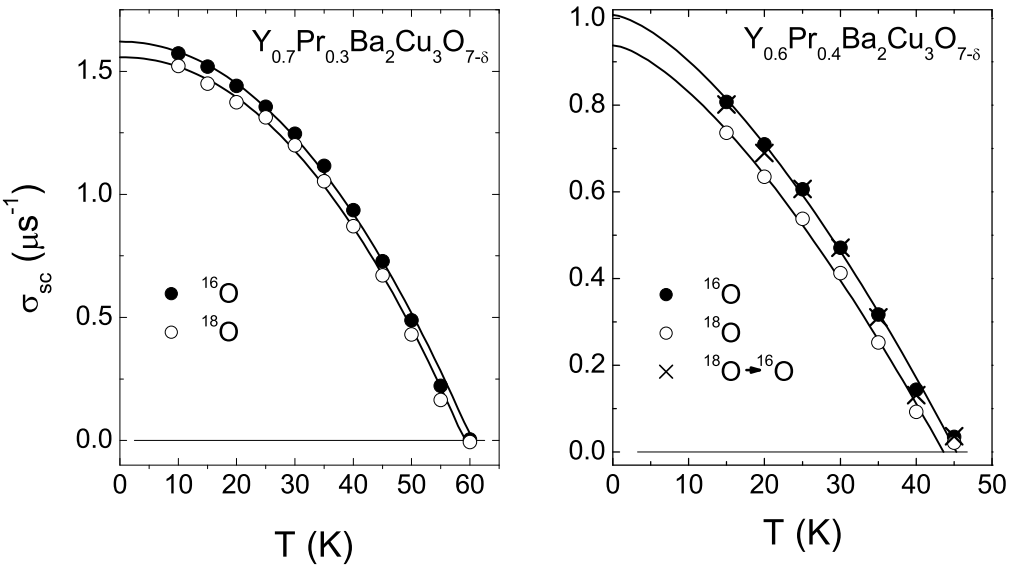

Figure 5. Temperature dependence of the μSR depolarization rate σ_{sc} of $Y_{1-x}Pr_xBa_2Cu_3O_{7-\delta}$ ($x = 0.3$ and $x = 0.4$) measured in a field 200 mT (FC). The error bars are smaller than the size of the data points. Data points below 10 K are not shown (see text for an explanation). The solid lines correspond to fits to the power law [see Eq. (7)]. After [20].

In Fig. 5 the temperature dependence of σ_{sc} for $Y_{1-x}Pr_xBa_2Cu_3O_{7-\delta}$ ($x = 0.3$ and $x = 0.4$) is shown. It is evident that for both concentrations x a remarkable oxygen isotope shift on T_c as well as on $\sigma_{sc}(0)$ is observed. The data in Fig. 5 were fitted to the power law [42]

$$\sigma_{sc}(T)/\sigma_{sc}(0) = 1 - (T/T_c)^n. \tag{7}$$

The values of $\sigma_{sc}(0)$ obtained from the fits were found to be in agreement with previous results [46]. In order to prove that the observed OIE on λ_{ab} is intrinsic, the ^{18}O sample with $x = 0.4$ was back exchanged (^{18}O→^{16}O). As seen in Fig. 5 the data points of this sample (crosses) coincide with those of the ^{16}O sample. From the measured values of $\sigma_{sc}(0)$ the relative isotope shift of $\lambda_{ab}(0)$ was found to be $\Delta\lambda_{ab}(0)/\lambda_{ab}(0) = 2.5(1)\%$ and $4.5(1)\%$ for $x = 0.3$ and $x = 0.4$ samples, respectively (see Table 1). For the OIE exponent $\beta_O = -d\ln\lambda_{ab}^{-2}/d\ln M_O$ one readily obtains $\beta_O = 0.38(12)$ for $x = 0.3$ and $\beta_O = 0.71(14)$ for $x = 0.4$. This means that in underdoped $Y_{1-x}Pr_xBa_2Cu_3O_{7-\delta}$ the OIE on $\lambda_{ab}^{-2}(0)$ as well on T_c increases with decreasing of doping. This is in excellent agreement with the magnetic torque results of underdoped $La_{2-x}Sr_xCuO_4$ single crystals [41].

Having established the existence of OIE on λ_{ab}, the following fundamental question arises: Which phonon modes are responsible for this effect? Insight in this respect can be obtained from studying the site-selective OIE (SOIE) on λ_{ab}. Khasanov *et al.* [21] performed detailed studies of the SOIE in underdoped $Y_{0.6}Pr_{0.4}Ba_2Cu_3O_{7-\delta}$ polycrystalline samples by bulk μSR. In a series of experiments ^{16}O (^{18}O) oxygen was selectively substituted by ^{18}O (^{16}O) at apical (a) and chain (c) sites, while ^{16}O (^{18}O) was kept at plane (p) sites, following the same procedure as described in Refs. [25, 24]. The site-selectivity of the oxygen exchange was checked by Raman spectroscopy [see Fig. 2 (b)]. Figure 6 shows the temperature dependence of the μSR depolarization rate

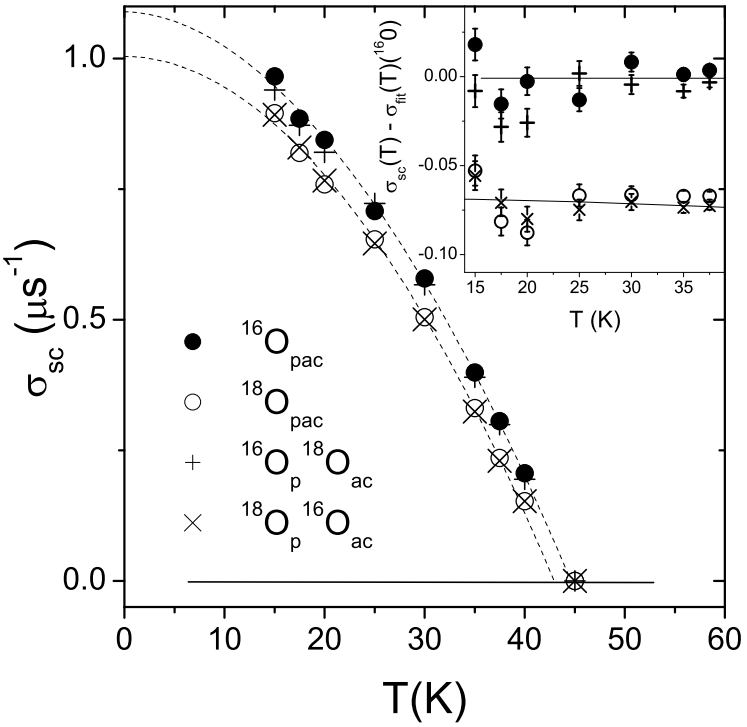

Figure 6. Temperature dependence of the depolarization rate σ_{sc} in site-selective $Y_{0.6}Pr_{0.4}Ba_2Cu_3O_{7-\delta}$ samples (200 mT, FC). Data points below 10 K are not shown (see text for an explanation). The solid lines correspond to fits to the power law $\sigma_{sc}(T)/\sigma_{sc}(0) = 1-(T/T_c)^n$ for the $^{16}O_{pac}$ and $^{18}O_{pac}$ samples. The inset shows data after subtracting the fitted curve for the $^{16}O_{pac}$ sample. After [21].

σ_{sc} for the $Y_{0.6}Pr_{0.4}Ba_2Cu_3O_{7-\delta}$ site-selective substituted samples. It is evident that a remarkable oxygen isotope shift of T_c as well as of σ_{sc} is present. More importantly, the data points of the site-selective $^{16}O_p{}^{18}O_{ac}$($^{18}O_p{}^{16}O_{ac}$) samples coincide with those of the $^{16}O_{pac}$($^{18}O_{pac}$) samples. In order to substantiate these results, the power law curve [Eq. (7)] fitting $\sigma_{sc}(T)$ for $^{16}O_{pac}$ was subtracted from the experimental data (inset

in Fig. 6). It can be seen that the experimental points for the two pairs of samples mentioned above coincide within error bar, indicating that the oxygen site within the CuO_2 planes mainly contribute to the total OIE on T_c and λ_{ab}.

4.2. OIE on λ_{ab} in optimally doped compounds

Recently, a substantial OIE on λ_{ab} in optimally doped samples of $YBa_2Cu_3O_{7-\delta}$ [$\Delta\lambda_{ab}(0)/\lambda_{ab}(0) = 2.6(5)\%$, $\beta_O = 0.41(7)$] (see Fig. 7) and $La_{1.85}Sr_{0.15}CuO_4$ [$\Delta\lambda_{ab}(0)/\lambda_{ab}(0) = 2.2(6)\%$, $\beta_O = 0.35(9)$] was observed by means of bulk μSR [47] (see Table 1). The observation of an OIE on λ_{ab} in optimally doped materials is remarkable considering the small OIE on T_c [$\Delta T_c/T_c = -0.26(5)\%$, $\alpha_O \simeq 0.03$]. The result is also in accordance with magnetization results obtained for optimally doped $Bi_{1.6}Pb_{0.4}Sr_2Ca_2Cu_3O_{10+\delta}$ [48].

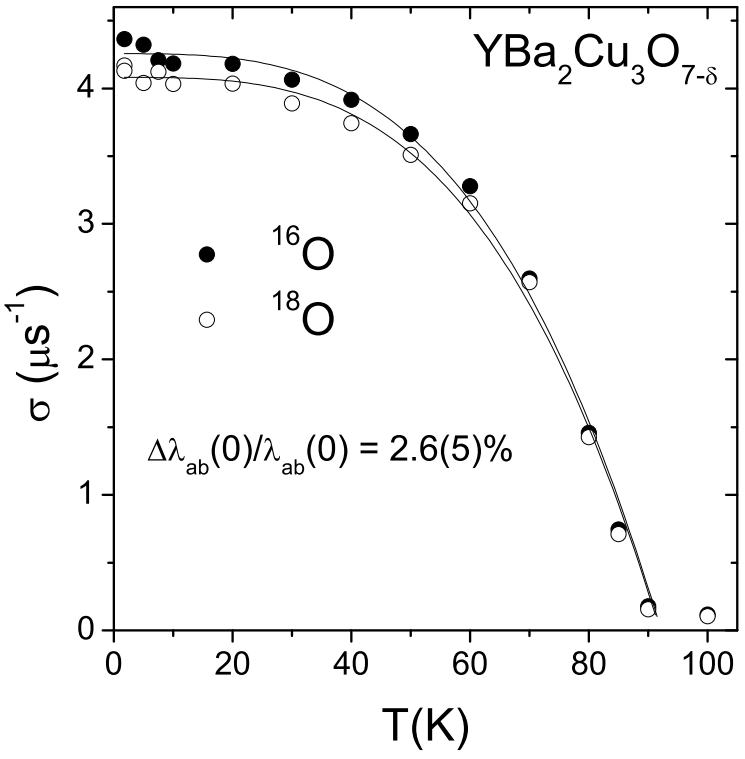

Figure 7. Temperature dependence of the μSR depolarization rate σ of oxygen isotope substituted $YBa_2Cu_3O_{7-\delta}$ measured in a field 200 mT (FC). The error bars are smaller than the size of the data points. The solid lines correspond to fits to the power law [Eq. (7)].

The most direct and model independent way to confirm this result is the determination of λ from the functional dependence of magnetic field profile $B(z)$

penetrating the surface of a superconductor in the Meissner state. Recently, such a measurement of λ_{ab} was performed in a thin film of $YBa_2Cu_3O_{7-\delta}$ at the Paul Scherrer Institute (PSI, Switzerland) [45] , by using the novel low-energy μSR (LEμSR) technique [49]. The principle of the measurement is shown schematically in Fig. 8. Polarized muons of energy in the keV range are implanted into the film. By tuning their energy these particles can be stopped at different and controllable depths beneath the surface of the superconductor in the Meissner state. The stopping profile of the muons, shown in the bottom part of Fig. 8(a), depends on the energy and can be reliably simulated [50, 51].

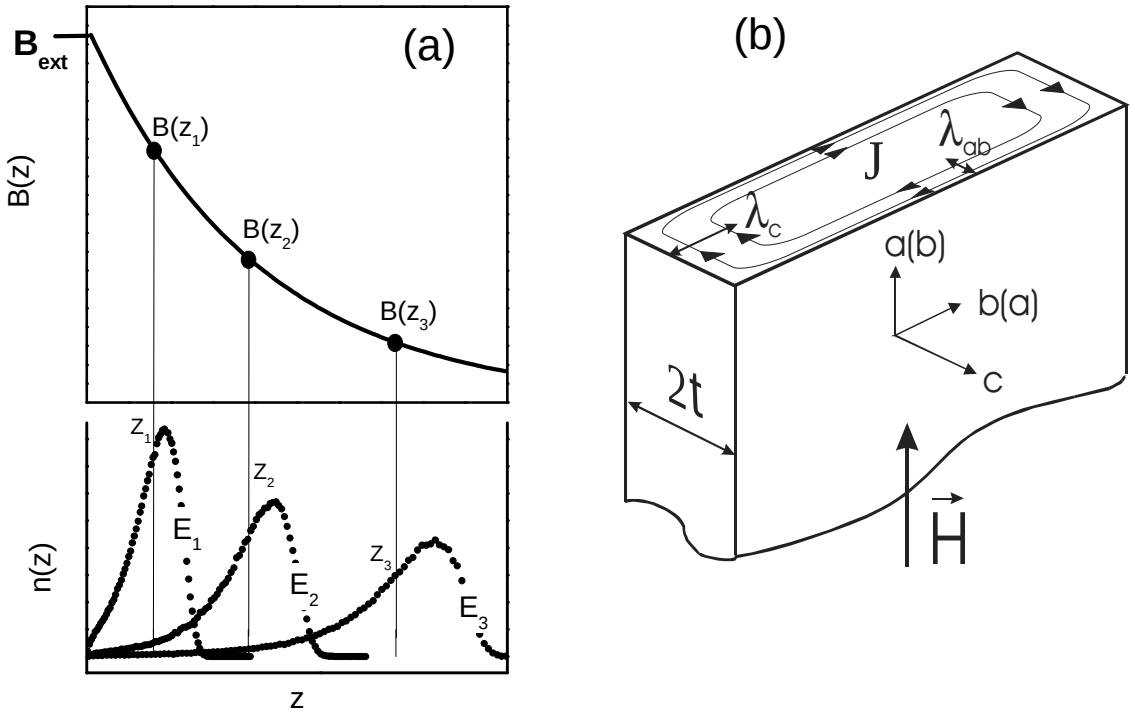

Figure 8. (a) Principle of λ determination by low-energy μSR. By tuning the energy of muons they are implanted at controllable distances ($\overline{z}_1$, $\overline{z}_2$, or $\overline{z}_3$) from the surface of the superconductor in a Meissner state. The local magnetic field $B(\overline{z})$ is determined from the muon precession frequency.(b) Schematic distribution of the screening current in a thin anisotropic superconducting slab of thickness $2t$ in a magnetic field applied parallel to the flat surface. The screening current J flows preferably parallel to the ab planes, giving rise to an exponential field decay along the crystal c-axis. Due to twinning in the ab planes (a and b axes are not distinguishable) the so called in-plane magnetic penetration depth λ_{ab} is measured.

By means of this technique, measurements of OIE on λ_{ab} in optimally doped c-axis oriented $YBa_2Cu_3O_{7-\delta}$ thin films were recently performed. A weak external magnetic field of 9.2 mT was applied parallel to the sample surface after the sample was cooled in

zero magnetic field from a temperature above T_c to 4 K. In this geometry (the thickness of the sample is negligible in comparison with the width), currents flowing in the *ab*-planes determine the magnetic field profile along the crystal *c*-axis inside the film [see Fig. 8(b)]. Spin-polarized muons were implanted at depths ranging from 20-150 nm beneath the surface of the film by varying the energy of the incident muons from 3 to 30 keV. For each implantation energy the average value of the magnetic field $\bar{B}$ and the

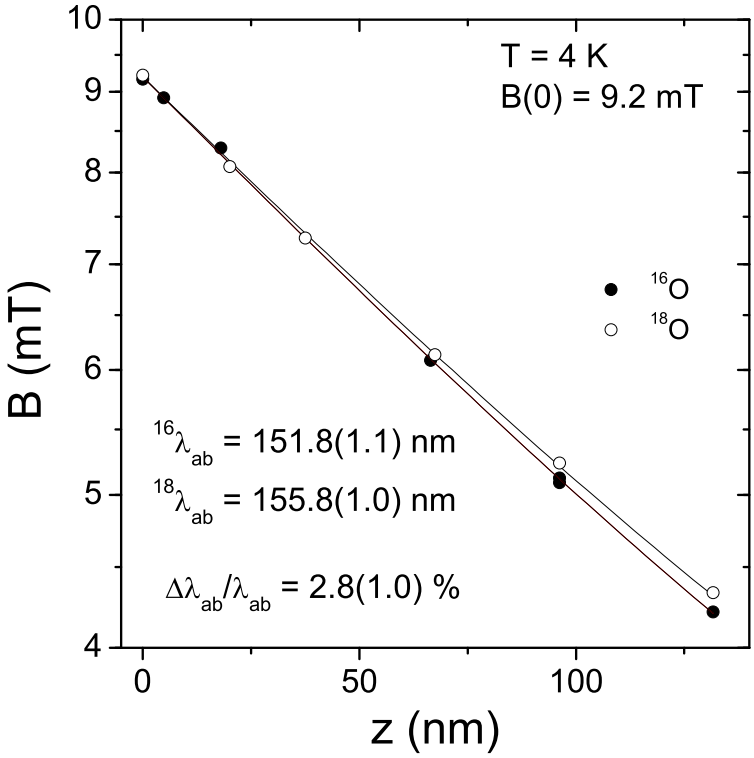

Figure 9. Magnetic field penetration profiles $B(z)$ on a logarithmic scale for a ^{16}O substituted (closed symbols) and a ^{18}O substituted (open symbols) $YBa_2Cu_3O_{7-\delta}$ film measured in the Meissner state at 4 K and an external field of 9.2 mT, applied parallel to the surface of the film. The data are shown for implantation energies 3, 6, 10, 16, 22, and 29 keV starting from the surface of the sample. Solid curves are best fits by Eq. (8). Error bars are smaller than the size of symbols. After [22].

correspondent average value of the stopping distance $\bar{z}$ were extracted. The value of $\bar{B}$ was taken from the fit of the time evolution of the muon-spin polarization spectrum by using the Gaussian relaxation function and $\bar{z}$ was the first moment of the simulated $n(z)$ distribution. Results of this analysis for the ^{16}O and ^{18}O substituted $YBa_2Cu_3O_{7-\delta}$ films are shown in Fig. 9. The magnetic penetration at the surface of the superconductor is more pronounced for the ^{18}O substituted film showing immediately that $^{18}\lambda_{ab} > ^{16}\lambda_{ab}$.

The solid lines represent a fit to the $\bar{B}$ data by the function:

$$B(z) = B(0)\frac{\cosh[(t-z)/\lambda_{ab}]}{\cosh(t/\lambda_{ab})} \; . \tag{8}$$

This is the form of the classical exponential field decay in the Meissner state $B(z) = B(0)\exp(-z/\lambda_{ab})$ (where $B(0)$ is the field at the surface of the superconductor), modified for a film with thickness $2t$ with flux penetrating from both sides. The value of z was corrected in order to take into account the surface roughness of the films [45], which was taken equal (8.0(5) nm) for both samples originating from the same batch. Fits with Eq. (8) to the extracted ${}^{16}\bar{B}(\bar{z})$ and ${}^{18}\bar{B}(\bar{z})$ yield ${}^{16}\lambda_{ab}(4\mathrm{K}) = 151.8(1.1)$ nm and ${}^{18}\lambda_{ab}(4\mathrm{K}) = 155.8(1.0)$ nm. Taking into account a ^{18}O content of 95%, the relative shift is found to be $\Delta\lambda_{ab}/\lambda_{ab} = ({}^{18}\lambda_{ab} - {}^{16}\lambda_{ab})/{}^{16}\lambda_{ab} = 2.8(1.0)\%$ at 4 K. This value is consistent with earlier estimates of the OIE on λ for optimally doped $YBa_2Cu_3O_{7-\delta}$ [39, 31], $La_{1.85}Sr_{0.15}CuO_4$ [48] and $Bi_{1.6}Pb_{0.4}Sr_2Ca_2Cu_3O_{10+\delta}$ [48] extracted *indirectly* from magnetization measurements.

In order to prove the intrinsic character of the effect, a backexchange experiment was performed on fine powder samples, where the isotope dependence of $\lambda_{ab}(0)$ can be determined from that of the Meissner fraction f [22]. Such type of measurements have been previously performed on the $La_{2-x}Sr_xCuO_4$ system in a wide range of doping ($0.06 \leq x \leq 0.15$) [16, 40]. Figure 10 shows the temperature dependence of λ_{ab}^{-2} calculated from f for the ${}^{16}O/{}^{18}O$ substituted $YBa_2Cu_3O_{7-\delta}$ fine powder samples. The value of f was determined from the FC SQUID magnetization measurements taken at 1 mT . The absence of weak links between grains is confirmed by the linear magnetic field dependence of the FC magnetization measured at 5 K in 0.5 mT, 1 mT, and 1.5 mT. $\lambda_{ab}(T)$ can be determined from the measured $\lambda_{\mathrm{eff}}(T)$ using the relation $\lambda_{\mathrm{eff}} = 1.31\lambda_{ab}$ which holds for highly anisotropic superconductors ($\lambda_c/\lambda_{ab} > 5$) [43, 44]. The relative shift at 4 K is found to be $\Delta\lambda_{ab}/\lambda_{ab} = 3.0(1.1)\%$, in good agreement with the bulk μSR and LEμSR data (see Figs. 7, 9 and Table 1). The results of the back exchange experiments shown as crosses in Fig. 10 prove the intrinsic character of the effect.

5. Implications of the OIE on λ_{ab} and universal correlations between OIE on T_c and λ_{ab}

From the present investigations it is evident that there is an OIE on $\lambda_{ab}(0)$ at all doping levels which appears to be generic for cuprate HTS. Here the fundamental questions arise: Is the observation of an OIE on the zero-temperature penetration depth (superfluid density) a direct signature of strong lattice effects? And what is the relevance of this finding for the pairing mechanism? In order to adequately answer these questions more experimental, and in particular more theoretical, work is needed. In the following we only discuss a few points related to these questions.

Under the assumption that we can *parameterize* experimental data of $\lambda_{ab}(0)$ in terms of Eq. (5) it follows from Eq. (6) that the isotope shift of λ_{ab} is due to an isotope shift of n_s and/or m_{ab}^*. It was demonstrated by a number of independent experiments

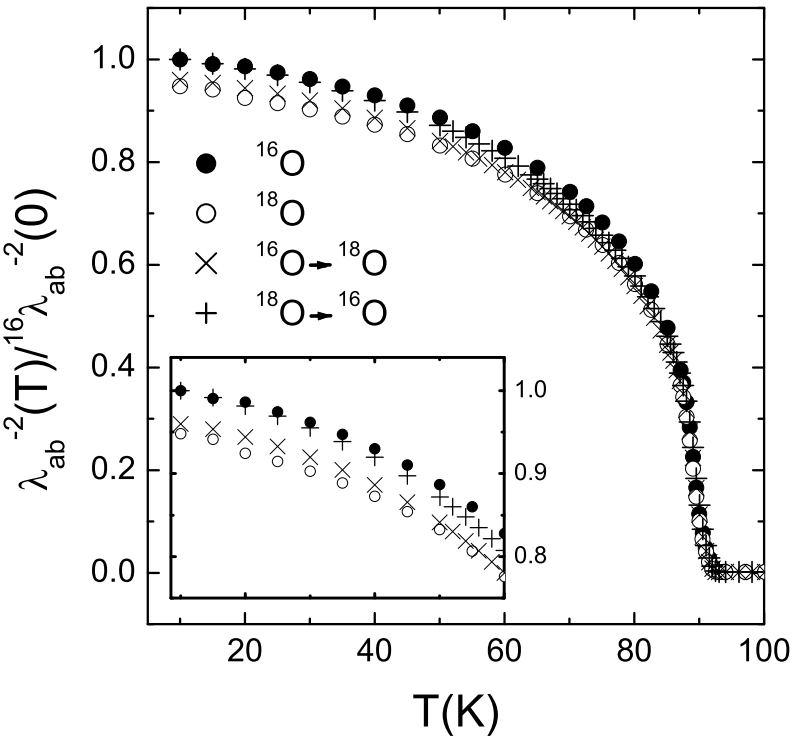

Figure 10. Temperature dependence of λ_{ab}^{-2} normalized by $^{16}\lambda_{ab}^{-2}(0)$ for ^{16}O and ^{18}O substituted $YBa_2Cu_3O_{7-\delta}$ fine powder samples as obtained from low-field SQUID magnetization measurements. The inset shows the low-temperature region between 10 K and 60 K. The reproducibility of the oxygen exchange procedure was checked by the backexchange (crosses). After [22].

that for $La_{2-x}Sr_xCuO_4$ [16, 18, 40, 41] and $Y_{1-x}Pr_xBa_2Cu_3O_{7-\delta}$ [20] the change of n_s during the oxygen exchange procedure is negligibly small. Recently, Khasanov *et al.* [22] provided further evidence of this scenario from measurements of the nuclear quadrupole resonance (NQR) frequency of the plane and the chain ^{63}Cu in ^{16}O and ^{18}O substituted optimally doped $YBa_2Cu_3O_{7-\delta}$ powder samples. It was found that the change of the hole number per unit cell caused by the isotope substitution is less than $\simeq 10^{-3}$. Since in optimally doped $YBa_2Cu_3O_{7-\delta}$ there is approximately one doped hole per unit cell, the relative change of the hole density $\Delta n/n$ at the oxygen exchange must be less than 10^{-3}. The absence of an observable OIE on n_s implies that the change of $\lambda_{ab}(0)$ is mainly due to a change on m_{ab}^*. From Eqs. (5) and (6) it follows that

$$\Delta m_{ab}^*/m_{ab}^* \simeq -\Delta\lambda_{ab}^{-2}(0)/\lambda_{ab}^{-2}(0) = 2\Delta\lambda_{ab}(0)/\lambda_{ab}(0). \qquad (9)$$

This implies that in HTS m_{ab}^* depends on the oxygen mass M_O with $\Delta m_{ab}^*/m_{ab}^* \simeq 5-10\%$, depending on doping level (see also Table 1). Note that such an isotope effect on m_{ab}^* is *not expected* for a conventional weak-coupling phonon-mediated BCS superconductor. In fact in HTS the charge carriers are very likely coupled to optical

phonons, as indicated by measurements of the static and high-frequency dielectric constants [52], neutron scattering [7, 8], photoemission [9, 10, 53] and tunnelling [54] experiments. Strong interaction between the charge carriers and the lattice ions leads to a *break down* of the adiabatic Migdal approximation [13], and consequently the effective supercarrier mass m^* depends on the mass of the lattice atoms. To our knowledge there are just a few theoretical models which predict an OIE on the effective carrier mass m^* (see *e.g.* Refs. [13, 55, 56, 57]).

Khasanov *et al.* [20] reported an empirical linear relation between the OIE exponents $\alpha_O = -d\ln T_c/d\ln M_O$ and $\beta_O = -d\ln\lambda_{ab}^{-2}(0)/d\ln M_O$ for underdoped $La_{2-x}Sr_xCuO_4$ and $Y_{1-x}Pr_xBa_2Cu_3O_{7-\delta}$. In Fig. 11 we plot $\Delta\lambda_{ab}(0)/\lambda_{ab}(0) \propto \beta_O$ versus $-\Delta T_c/T_c \propto \alpha_O$ for $Y_{1-x}Pr_xBa_2Cu_3O_{7-\delta}$ and $La_{2-x}Sr_xCuO_4$ for the data listed in Table 1. It is evident from Fig. 11 that there is correlation between the OIE of T_c and $\lambda_{ab}(0)$ which appears to be universal for cuprate HTS. Different experimental techniques (SQUID magnetization, magnetic torque, bulk μSR, LEμSR) and different types of samples (single crystals, powders, thin films) yield within error bar consisting results, indicating that the observed *isotope effects are intrinsic* and not artifacts of the particular experimental method or sample used. As indicated by the dashed line, at low doping level $\Delta\lambda_{ab}(0)/\lambda_{ab}(0) \simeq |\Delta T_c/T_c|$, whereas close to optimal doping $\Delta\lambda_{ab}(0)/\lambda_{ab}(0)$ is almost constant and considerably larger than $|\Delta T_c/T_c|$ ($\Delta\lambda_{ab}(0)/\lambda_{ab}(0) \approx 10|\Delta T_c/T_c|$). This finding is consistent with the empirical "Uemura relation" [58, 59] and with the "parabolic ansatz" proposed in [30] in a *differential way* for doped cuprate HTS.

It was shown by Schneider and Keller [60, 61] that this empirical relation naturally follows from the doping driven 3D-2D crossover and the 2D quantum superconductor to insulator (2D-QSI) transition in the highly underdoped limit. Close to the 2D-QSI transition the following relation holds [61]:

$$\Delta\lambda_{ab}(0)/\lambda_{ab}(0) = (1/2)[\Delta d_s/d_s - \Delta T_c/T_c], \tag{10}$$

where $\Delta d_s/d_s$ is the oxygen-isotope shift of the thickness of the superconducting sheets d_s of the sample. The solid line in Fig. 11 represents a best fit of Eq. (10) to the data with $\Delta d_s/d_s = 3.3(4)\%$. Since the lattice parameters are not modified by oxygen substitution [62, 63], the observation of an isotope shift of d_s implies local lattice distortions involving oxygen which are coupled to the superfluid [61].

As shown in Fig. 12, a similar type of correlation between the OIE on $\lambda_{ab}(0)$ and OIE on T_c is also observed for the site-selective substituted $Y_{0.6}Pr_{0.4}Ba_2Cu_3O_{7-\delta}$ samples [21]. It is evident that the oxygen site within the CuO_2 planes mainly contributes to the total OIE on T_c and $\lambda_{ab}(0)$. Since for fixed Pr concentration the lattice parameters remain essentially unaffected by the isotope substitution [62, 63], these results unambiguously demonstrate the existence of a coupling of the charge carriers to phonon modes involving movements of the oxygen atoms in the CuO_2 plane, while suggesting that modes involving apical and chain oxygen are less strongly coupled to the carriers.

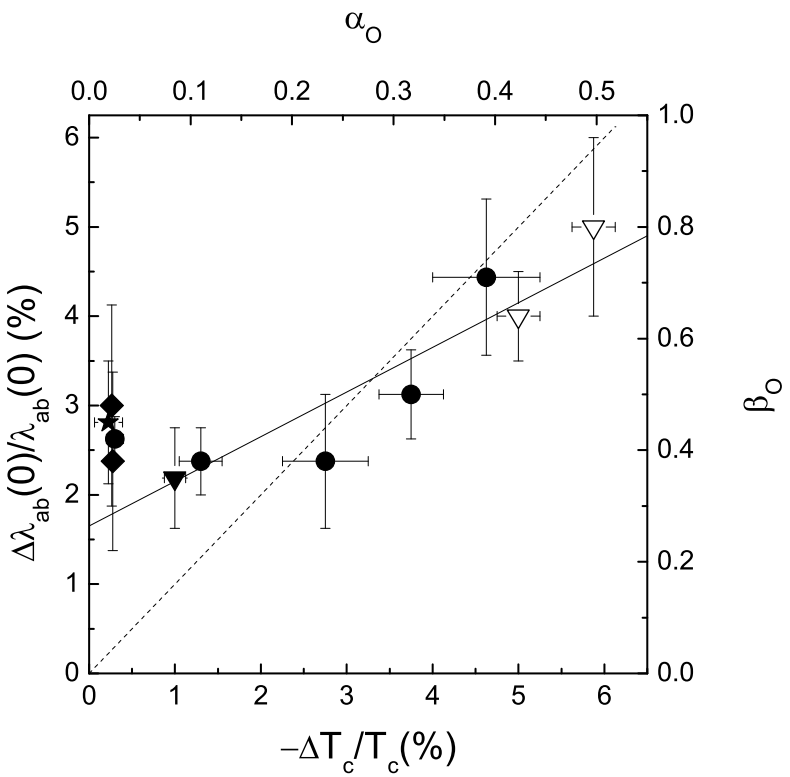

Figure 11. Plot of the OIE shift $\Delta\lambda_{ab}(0)/\lambda_{ab}(0)$ (OIE exponent $\beta_{\rm O}$) versus the OIE shift $-\Delta T_c/T_c$ (OIE exponent $\alpha_{\rm O}$) for $Y_{1-x}Pr_xBa_2Cu_3O_{7-\delta}$ and $La_{2-x}Sr_xCuO_4$. Closed circles and triangles are bulk μSR data for $Y_{1-x}Pr_xBa_2Cu_3O_{7-\delta}$ and $La_{1.85}Sr_{0.15}CuO_4$ (Table 1). Diamonds and stars are LEμSR and Meissner fraction data for optimally doped $YBa_2Cu_3O_{7-\delta}$ (Table 1). Open triangles are torque magnetization data for $La_{2-x}Sr_xCuO_4$ from [41]. The dashed line corresponds to $\Delta\lambda_{ab}(0)/\lambda_{ab}(0) = |\Delta T_c/T_c|$. The solid line indicates the flow to 2D-OSI criticality and provides with Eq. (10) an estimate for the oxygen isotope effect on d_s, namely $\Delta d_s/d_s = 3.3(4)\%$.

6. Conclusions

In conclusion, the unconventional isotope effects presented here clearly demonstrate that lattice effects play an important role in the physics of cuprates. The fact that a substantial OIE on λ_{ab} is observed, even in optimally doped cuprates, strongly suggests that cuprate HTS are *non-adiabatic* superconductors. This is in contrast to the novel high-temperature superconductor MgB_2 for which within experimental error no Boron ($^{10}B/^{11}B$) isotope effect on the magnetic penetration depth was detected [64]. The site-selective OIE studies of T_c and λ_{ab} indicate that the phonon modes involving the movements of oxygen within the superconducting CuO_2 planes are essential for the occurrence of superconductivity in cuprate HTS. This is in agreement with

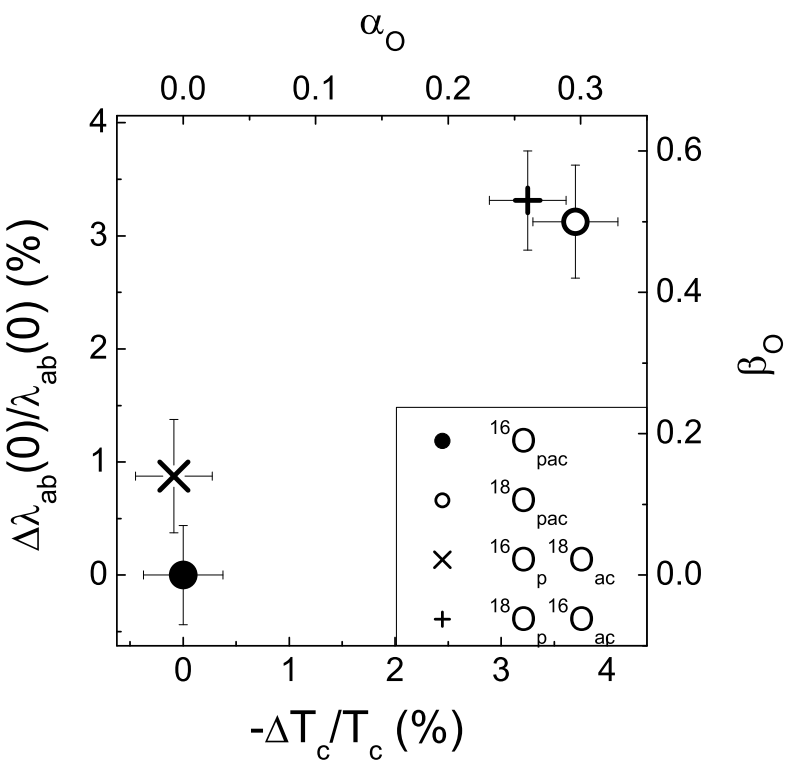

Figure 12. Plot of the OIE shift of the in-plane penetration depth $\Delta\lambda_{ab}(0)/\lambda_{ab}(0)$ (OIE exponent $\beta_{\rm O}$) versus the OIE shift of the transition temperature -$\Delta T_c/T_c$ (OIE exponent $\alpha_{\rm O}$) for site-selective substituted $Y_{0.6}Pr_{0.4}Ba_2Cu_3O_{7-\delta}$ samples. The error bars of the "trivial" $^{16}O_{\rm pac}$ point (zero isotope shift by definition) indicate the intrinsic uncertainty in the determination of T_c and λ_{ab}. After [21].

recent inelastic neutron scattering [7, 8] and photoemission [9, 10] studies, indicating a strong interaction between charge carriers and Cu-O bond-stretching-type of phonons. The generic relation between the OIE on T_c and λ_{ab} demonstrates that, in contrast to conventional phonon-mediated superconductors, λ_{ab} (superfluid density) is a key parameter for understanding the role of phonons in cuprates, in particular local lattice distortions involving planar oxygen. The present results rise serious doubts that models, neglecting lattice degrees of freedom, as proposed for instance in [65], are potential candidates to explain superconductivity in HTS.

This work was partly performed at the Swiss Muon Source (SμS), Paul Scherrer Institute (PSI, Switzerland). The authors are grateful to A. Amato U. Zimmermann, and D. Herlach for help during the μSR measurements, D. Di Castro, N. Garifianov, D.G. Eshchenko, H. Luetkens, T. Prokscha, and A. Suter for helpful discussions and participating in some μSR experiments, A. Bussmann-Holder, E. Liarokapis,

D. Lampakis, M. Mali, K.A. Müller, J. Roos, T. Schneider, Z.-X. Shen, A. Tatsi, and G.M. Zhao for their collaborations and discussions. This work was supported by the Swiss National Science Foundation and by the NCCR program *Materials with Novel Electronic Properties* (MaNEP) sponsored by the Swiss National Science Foundation.

References

[1] Bednorz J G and Müller K A 1986 *Z. Phys. B* **64** 189
[2] Batlogg B, Cava R J, Jayaraman A, van Dover R B, Kourouklis G A, Sunshine S, Murphy D W, Rupp L W, Chen H S, White A, Short K T, Mujsce A M, and Rietman E A 1986 *Phys. Rev. Lett.* **58** 2333
[3] Batlogg B, Kourouklis G, Weber W, Cava R J, Jayaraman A, White A E, Short K T, Rupp L W, and Rietman E A 1887 *Phys. Rev. Lett.* **59** 912
[4] Bourne L C, Crommie M F, Zettl A, Hans-Conrad zur Loye, Keller S W, Leary K L, Stacy Angelica M Chang K J, Cohen Marvin L, and Morris Donald E 1987 *Phys. Rev. Lett.* **58** 2337
[5] Carbotte J P, 1990 *Rev. Mod. Phys.* **62** 1027
[6] Nagamatsu J, Nakagawa N, Muranaka T, Zenitani Y, and Akimitsu J 2001 *Nature (London)* **410** 63
[7] McQueeney R J, Sarrao J L, Pagliuso P G, Stephens P W, and Osborn R 1999 *Phys. Rev. Lett.* **82** 628; 2001 **87** 077001; d'Astuto M, Mang P K, Giura P, Shukla A, Ghigna P, Mirone A, Braden M, Greven M, Krisch M, and Sette F 2002 *ibid.* **88** 167002
[8] Chung J-H, Egami T, McQueeney R J, Yethiraj M, Arai M, Yokoo T, Petrov Y, Mook H A, Endoh Y, Tajima S, Frost C, and Dogan F 2003 *Phys. Rev. B* **67** 014517
[9] Bogdanov P V, Lanzara A, Kellar S A, Zhou X J, Lu E D, Zheng W J, Gu G, Shimoyama J-I, Kishio K, Ikeda H, Yoshizaki R, Hussain Z, and Shen Z- 2000 *Phys. Rev. Lett.* **85** 2581; Bogdanov P V, Lanzara A, Zhou X J, Yang W L, Eisaki H, Hussain Z, and Shen Z-X 2002 *ibid.* **89** 167002
[10] Lanzara A, Bogdanov P V, Zhou X J, Kellar S A, Feng D L, Lu E D, Yoshida T, Eisaki H, Fujimori A, Kishio K, Shimoyama J-I, Noda T, Uchida S, Hussain Z, and Shen Z-X 2001 *Nature (London)* **412** 510
[11] Bussmann-Holder A, Müller K A, Micnas R, Büttner H, Simon A, Bishop A R, and Egami T 2001 *J. Phys.: Condens. Matter* **13** L169; Mihailovic D and Kabanov V V 2001 *Phys. Rev. B* **63** 054505; Shen Z-X *et al.* 2002 *Phil. Mag. B* **82** 1349; Tachiki M, Machida M, and Egami T 2003 *Phys. Rev. B* **67** 174506
[12] Eschrig M and Norman M R 2003 *Phys. Rev. B* **67** 144503; Schachinger E, Tu J J, and Carbotte J P 2003 *ibid.* **67** 214508
[13] Alexandrov A S and Mott N F 1994 *Int. J. Mod. Phys.* **8** 2075
[14] Müller K A 1900 *Z. Phys. B.* **80** 193
[15] Zech D, Conder K, Keller H, Kaldis E, Liarokapis E, Poulakis N, and Müller K A, *in: Anharmonic Properties of High-T_c Cuprates*, ed. D. Mihailović, G. Ruani, E. Kaldis, and K.A. Müller (World Scientific, Singapore, 1995), pp. 18-29.
[16] Zhao G M, Conder K, Keller H, and Müller K A 1998 *J. Phys.: Condens. Matter* **10** 9055
[17] Müller K A 2000 *Physica C* **341-348** 11
[18] Zhao G M, Keller H, and Conder K 2001 *J. Phys.: Cond. Matter* **13** R569
[19] Keller H 2003 *Physica B* **326** 283
[20] Khasanov R, Shengelaya A, Conder K, Morenzoni E, Savić I M, and Keller H 2003 *J. Phys.: Condens Matter* **15** L17
[21] Khasanov R, Shengelaya A, Morenzoni E, Angst M, Conder K, Savić I M, Lampakis D, Liarokapis E, Tatsi A, and Keller H 2003 *Phys. Rev. B* **68** 220506

[22] Khasanov R, Eshchenko D G, Luetkens H, Morenzoni E, Prokscha T, Suter A, Garifianov N, Mali M, Roos J, Conder K, and Keller H 2004 *Phys. Rev. Lett.* **92** 057602
[23] Morenzoni E, Prokscha Th, Hofer A, Matthias B, Meyberg M, Wutzke Th, Glckler H, Birke M, Litterst J, Niedermayer Ch, Schatz G 1997 *J. Appl. Phys.* **81** 3340
[24] Conder K 2001 *Mater. Sci. Eng.* **R32** 41
[25] Zech D, Keller H, Conder K, Kaldis E, Liarokapis E, Poulakis N, and Müller K A 1994 *Nature (London)* **371** 681
[26] Ramirez A P, Kortan A R, Rosseinsky M J, Duclos S J, Mujsce A M, Haddon R C, Murphy D W, Makhija A V, Zahurak S M, and Lyons K B 1992 *Phys. Rev. Lett.* **68** 1058
[27] Budko S L, Lapertot G, Petrovic C, Cunningham C E, Anderson N, and Canfield P C 2001 *Phys. Rev. Lett.* **86** 1877; Hinks D G, Claus H, and Jorgensen J D 2001 *Nature (London)* **411** 457
[28] Franck J P, Jung J, Mohamed M A-K, Gygax S, and Sproule G I 1991 *Phys. Rev. B* **44** 5318
[29] Franck J P, in: *Physical Properties of High Temperature Superconductors IV*, edited by D. M. Ginsberg (World Scientific, Singapore, 1994), pp. 189–293
[30] Schneider T and Keller H 1992 *Phys. Rev. Lett.* **69** 3374
[31] Zhao G M and Morris D E 1996 *Phys. Rev. B* **51** 14982
[32] Bornermann H J and Morris D E 1991 *Phys. rev. B* **44** 5532
[33] Babushkina N, Inyushkin A, Ozhogin V, Taldenkov A, Kobrin I, Vorob'eva T, Molchanova L, Damyanets L, Uvarova T, and Kuzakov A 1991 *Physica C* **185-189** 901
[34] Franck J P, Harker S, and Brewer J 1993 *Phys. Rev. Lett.* **71** 283
[35] Zhao G M, Kirtikar V, Singh K K, Sinha A P B, Morris Donald E, and Inyushkin A V 1996 *Phys. Rev. B* **54** 14956
[36] Morris D E, Sinha A P B, Kirtikar V, and Inyushkin A V 1998 *Physica C* **298** 203
[37] Williams G V M, Pringle D J, and Tallon J L 2000 *Phys. Rev. B* **61** R9257
[38] Chandrasekhar B S and Einzel D 1993 *Ann. Physik* **2** 535
[39] Zhao G M and Morris D E 1995 *Phys. Rev. B* **51** 16487
[40] Zhao G. M, Hunt M B, Keller H, and Müller K A 1997 *Nature (London)* **385** 236
[41] Hofer J, Conder K, Sasagawa T, Zhao G M, Willemin M, Keller H, and Kishio K 2000 *Phys. Rev. Lett.* **84** 4192
[42] Zimmermann P, Keller H, Lee S L, Savic I M, Warden M, Zech D, Cubitt R, Forgan E M, Kaldis E, Karpinski J, and Krüger C 1995 *Phys. Rev. B* **52** 541
[43] Barford W and Gunn J M F 1988 *Physica C* **156** 515
[44] Fesenko V I, Gorbunov V N, and Smilga V P 1991 *Physica C* **176** 551
[45] Jackson T J, Riseman T M, Forgan E M, Glückler H, Prokscha T, Morenzoni E, Pleines M, Niedermayer Ch, Schatz G, Luetkens H, and Litterst J 2000 *Phys. Rev. Lett.* **84** 4958
[46] Seaman C L, Neumeier J J, Maple M B, Le L P, Luke G M, Sternlieb B J, Uemura Y J, Brewer J H, Kadono R, Kiefl R F, Krietzman S R, and Riseman T M 1990 *Phys. Rev. B* **42** 6801
[47] Khasanov R *et al.* unpublished.
[48] Zhao G M, Kirtikar Vidula, and Morris Donald E 2001 *Phys. Rev. B* **63** 220506
[49] Morenzoni E, Kottmann F, Maden D, Matthias B, Meyberg M, Prokscha Th, Wutzke Th, and Zimmermann U 1994 *Phys. Rev. Lett.* **72** 2793
[50] Morenzoni E, Glückler H, Prokscha T, Khasanov R, Luetkens H, Birke M, Forgan E M, and Niedermayer Ch 2002 *Nucl. Instr. Meth. B* **192** 254
[51] Morenzoni E, Prokscha T, Suter A, Luetkens H, and Khasanov R (in this issue).
[52] Alexandrov A S and Bratkovsky A M 2000 *Phys. Rev. Lett.* **84** 2043
[53] Shen Z-X, Lanzara A, Ishihara S, Nagaosa N, cond-mat/0108381.
[54] Ponomarev Ya G, Tsokur E B, Sudakova M V, Tchesnokov S N, Shabalin M E, Lorenz M A, Hein M A, Müller G, Piel H, and Aminov B A 1999 *Solid State Commun.* **111** 513
[55] Scalapino D J, Scalettar R T, and Bickers N E, in *Proceedings of the International Conference on Novel Mechanisms of Superconductivity, New York, 1987,* edited by S.E Wolf and V.Z. Kresin

(Plenum, New York, 1987), p. 475
[56] Grimaldi C, Cappelluti E, and Pietronero L 1998 *Europhys. Lett.* **42** 667
[57] Bussmann-Holder A and Micnas R 2002 *J. Supercond.* **15** 321
[58] Uemura Y J, Luke G M, Sternlieb B J, Brewer J H, Carolan J F, Hardy W N, Kadono R, Kempton J R, Kiefl R F, Kreitzman S R, Mulhern P, Riseman T M, Williams D Ll, Yang B X, Uchida S, Takagi H, Gopalakrishnan J, Sleight A W, Subramanian A M, Chien C L, Cieplak M Z, Gang Xiao, Lee V Y, Statt B W, Stronach C E, Kossler W J, and Yu X H 1989 *Phys. Rev. Lett.* **62** 2317
[59] Uemura Y J, Le L P, Luke G M, Sternlieb B J, Wu W D, Brewer J H, Riseman T M, Seaman C L, Maple M B, Ishikawa M, Hinks D G, Jorgensen J D, Saito G, and Yamochi H 1991 *Phys. Rev. Lett.* **66** 2665
[60] Schneider T and Keller H 2001 *Phys. Rev. Lett.* **86** 4899
[61] Keller H and Schneider T cond-mat/0401505.
[62] Conder K, Zech D, Krüger Ch, Kaldis E, Keller H, Hewat A W, and Jilek E, in *Phase Separation in Cuprate Superconductors*, edited by E. Sigmund and K. A. Müller (Springer, Berlin 1994) p. 210
[63] Raffa F, Ohno T, Mali M, Roos J, Brinkmann D, Conder K, and Eremin M 1998 *Phys. Rev. Lett.* **81** 5912
[64] Di Castro D, Angst M, Eshchenko D G, Khasanov R, Roos J, Savić I M, Shengelaya A, Bud'ko S L, Canfield P C, Conder K, Karpinski J, Kazakov S M, Ribeiro R A, and Keller H, cond-mat/0307330
[65] Anderson P W, Lee P A, Randeria M, Rice T M, Trivedi N, and Zhang F C, cond-mat/0311467